



ELSEVIER

Journal of Chromatography A, 822 (1998) 326–331

JOURNAL OF
CHROMATOGRAPHY A

Short communication

Gas–solid chromatographic separation of hydrogen isotopes: a comparison between two palladium bearing materials – alumina and kieselguhr

Françoise Strzelczyk^a, Didier Leterq^b, A.M. Wilhelm^c, Alexis Steinbrunn^{a,*}

^aLaboratoire de Recherches sur la Réactivité des Solides – CNRS U.M.R 5613, Université de Bourgogne – UFR Sciences et Techniques 9, Avenue Alain Savary, B.P 400, 21011 Dijon Cedex, France

^bCEA Centre d'Études de Valduc, 21120 Is sur Tille, France

^cENSIGC, Chemin de la Loge, 31078 Toulouse Cedex, France

Received 15 April 1998; received in revised form 21 July 1998; accepted 27 July 1998

Abstract

The separation of hydrogen isotopes (H, D, T) is performed by displacement gas chromatography on palladium. A large isotopic effect is associated with the reversible adsorption of hydrogen by palladium. Two Pd support materials have been compared: alpha-alumina and kieselguhr. The study includes a physicochemical characterization and a set of functional tests. The Van Deemter model gives a fairly good analysis of the process but to get more information, thermoregulated separations are needed. For both supports, palladium is impregnated as small dispersed particles in the 0.1 to 0.3 μm range diameter. For the same palladium loading, alumina is more efficient than kieselguhr. © 1998 Elsevier Science B.V. All rights reserved.

Keywords: Palladium support materials; Stationary phases, GC; Hydrogen; Deuterium; Tritium

1. Introduction

The separation of hydrogen isotopes (H, D, T) is performed by displacement gas chromatography on palladium. Palladium is loaded with the mixture to process, then this mixture is displaced by pure protium. The isotope with the lowest affinity for the palladium will arrive first at the column exit: tritium is the first one, followed by deuterium and finally protium [1–3].

In order to obtain practical exchange rates in hydride-based systems, the characteristic dimension

of the metal particles must be no more than a few microns. As a separation column packed with such material would have unacceptably low permeability, the metal must be dispersed in some way on larger particles [4]. Two support materials have been studied: alpha-alumina and kieselguhr.

This study includes a physicochemical characterization of both supports and a set of functional tests. The Van Deemter model, which is suitable to qualify the packing material efficiency, is considered as a fast and a fairly good means to analyse our process. This work allows us to identify the better packing material as well as to optimize the separation process.

*Corresponding author.

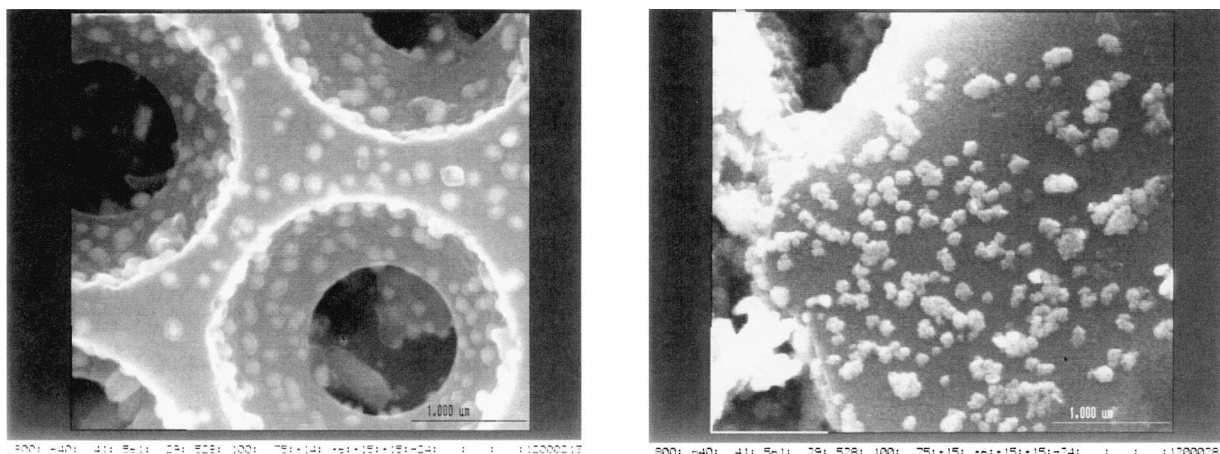


Fig. 1. SEM micrographs (25 000 \times) of kieselguhr (left) and alumina (right) both impregnated with 20% palladium.

2. Experimental

2.1. Materials

The palladium impregnation was performed by Johnson Matthey (UK) by immersing both porous supports, kieselguhr and alumina, into a palladium salt solution (whose nature is kept confidential). The kieselguhr is a diatomaceous earth mainly constituted of silica (90% SiO₂–10% Al₂O₃). The alumina used in this study is alpha-alumina (corundum). They were delivered by Manville Sales (USA) and Société des Céramiques de Tarbes, respectively. The average grain size is 1 mm and 0.3 mm for alumina and kieselguhr, respectively. For each material support, two palladium contents were studied: 20 and 30% (w/w). The palladium contents were analyzed by inductively coupled plasma atomic energy spectrometry (ICP-AES): they are in good agreement with the expected palladium loadings.

The palladium structure and its morphology have been analyzed by transmission electron microscopy (TEM) and scanning electron microscopy (SEM).

High magnifications and SEM backscattered electrons mode are needed to reveal the distribution of palladium islands at the support surfaces. For each support material, palladium looks like uniformly dispersed particles of 0.1 to 0.3 μm size (Fig. 1). Electron microdiffraction analyses by TEM showed that it is well crystallized into a face-centered cubic lattice (*fcc*) whose unit cell is equal to 0.39 nm.

The specific surface area of each packing material was determined by the Brunauer Emmet Teller (BET) method (Micromeritics Autosor 1). Krypton was used to evaluate the specific surface area of alumina without palladium, instead of nitrogen which was mainly used for other packing materials. The experimental values are summarized in Table 1.

The specific surface area (*S*) increases with the palladium content. This result suggests a palladium distribution in the form of small particles which is in agreement with the SEM analyses.

The porosity (ϵ) as well as the average pore size (ϕ) were evaluated by mercury porosimetry (Micromeritics Pore Sizer 9320). The experimental values are expressed in Table 2.

Table 1
Alumina and kieselguhr specific surface area.

	Al ₂ O ₃	Al ₂ O ₃ +20% Pd	Al ₂ O ₃ +30% Pd	Kieselguhr	Kieselguhr+20% Pd	Kieselguhr+30% Pd
<i>S</i> (m ² /g)	0.51	1.2	1.49	3.6	3.7	3.5

Table 2
Mercury porosimetry measurements

	Al ₂ O ₃	Al ₂ O ₃ +20% Pd	Al ₂ O ₃ +30% Pd	Kieselguhr	Kieselguhr+20% Pd	Kieselguhr+30% Pd
ε (%)	72	70	66	82.2	75.6	76
ϕ (μm)	1.29	1.22	1.04	0.9	0.84	0.84

The porosity weakly decreases when the palladium content increases. The weak variations of the pore diameter confirms the small sized palladium islands as observed by SEM analyses.

2.2. Chromatography apparatus and experimental procedure

The equipment used to perform the functional tests is composed of a stainless steel tube column (2.05 m×9.4 mm I.D.). It is equipped with a three-way valve, pressure transducers, a mass flow meter and a catharometer. Dead volumes will be reduced to limit the external contributions. These latter values will be determined by means of a bypass (Fig. 2).

The experimental procedure is composed of the following steps at room temperature: (i) activation of the packing material, which is achieved by several hydrogenation–dehydrogenation cycles at room temperature until hydride saturation (PdH_{0.7}) is obtained. (ii) Loading of the mixture to separate into the column until the catharometer signal is stable. (iii) Elution by pure protium.

The mean pressure in the column is maintained at 1 bar and the flow-rate is regulated by the micrometric valve at the output of the column. The elution is performed for several flow-rates through the column and by bypassing the column.

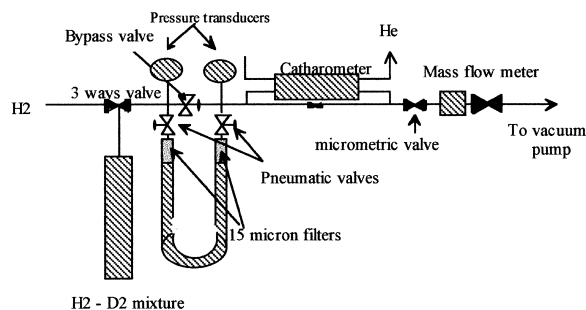


Fig. 2. Chromatography apparatus.

In order to be able to use the Van Deemter model, the mixture composition H₂–D₂ (93:7) has been chosen for this study.

3. Results and discussion

For each flow-rate, the height equivalent to a theoretical plate (HETP) is deduced from the breakthrough curve. By plotting the HETP as a function of the interstitial gas velocity, U , the Van Deemter curves are obtained (Fig. 3).

The experimental curves are in a fairly good agreement with the characteristic Van Deemter equation, $A+B/U+CU$. Our results are summarized in Table 3.

It is worthwhile to underline that the lower the HETP is, the better the separation efficiency is.

Whatever the palladium content, alumina is more efficient than kieselguhr. For a given support material, an additional charge in palladium improves the separation efficiency.

3.1. The Van Deemter model

This model is commonly used to describe the separation process. It is suitable only for a linear adsorption isotherm. The linearity is checked by the comparison between the shape of a direct breakthrough curve and that of the reverse one. These two curves should be similar. The direct separation consists in an elution performed by pure protium (the column is initially saturated by the mixture), while the reverse separation takes place when the elution is carried out by the mixture (the column is then saturated by pure protium) [5–7]. Various experiments with several D₂ contents have been achieved. The composition of mixture corresponding to the best of the previous considerations is H₂–D₂ (93:7).

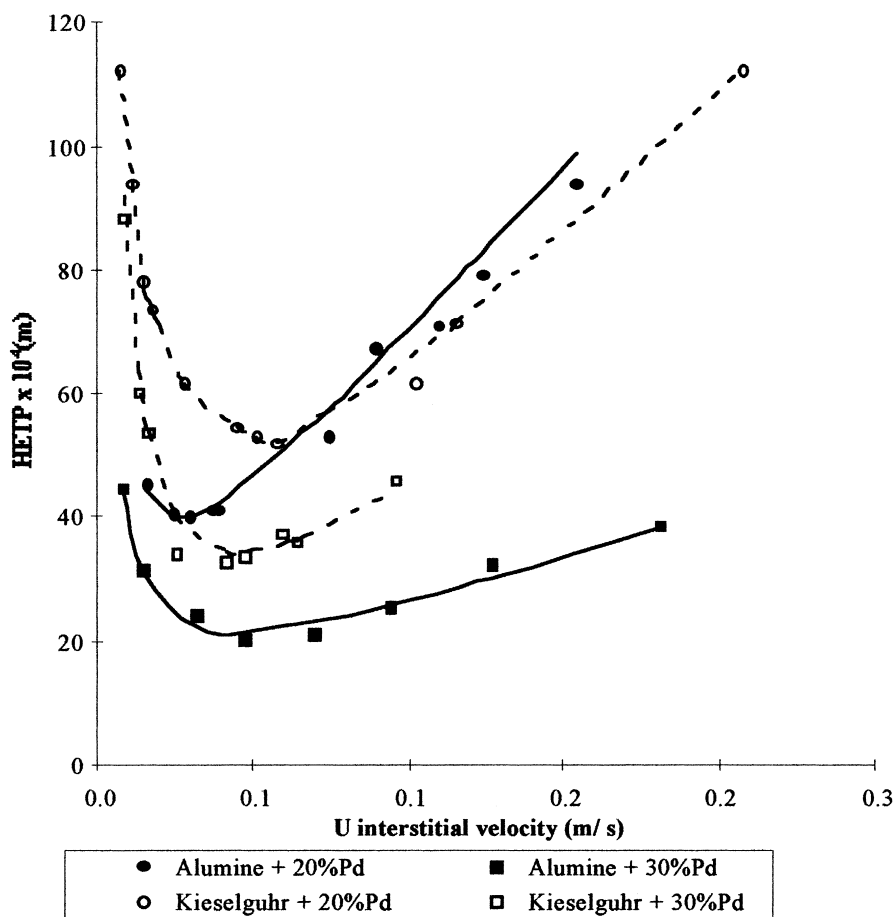


Fig. 3. Van Deemter curves deduced from a mixture (93% H₂–7% D₂) separation on alumina and kieselguhr coated by palladium.

So have we decided to use it for our study. For a non-linear isotherm, effects of dispersive and compressive breakthrough appear [5–7].

The Van Deemter model gives the HETP as a

function of the interstitial gas velocity (*U*) whose general equation is:

$$HETP = A + B/U + CU$$

Table 3
Van Deemter curve equations as a function of the palladium content and for each support material

	Al ₂ O ₃ + 20% Pd	Al ₂ O ₃ + 30% Pd
HETP=f(U)	HETP=4·10 ⁻⁴ /U + 10 ⁻³ + 5.6·10 ⁻³ U H _{min} =4.0·10 ⁻³ m	HETP=3.1·10 ⁻⁴ /U + 7·10 ⁻⁴ + 1.62·10 ⁻³ U H _{mini} =2.0·10 ⁻³ m
	Kieselguhr + 20% Pd	Kieselguhr + 30% Pd
HETP=f(U)	HETP=8.9·10 ⁻⁴ /U + 7·10 ⁻⁴ + 4.78·10 ⁻³ U H _{min} =5.0·10 ⁻³ m	HETP=7.8·10 ⁻⁴ /U + 3.75·10 ⁻³ U H _{min} =3.4·10 ⁻³ m

where the coefficients A , B , C refer to mechanical dispersion, molecular diffusion and mass transfer, respectively.

This equation results from a mass balance in a column section for both gas- and solid-phases [5,8–12] and allows one to determine the optimum flow-rate and to quantify the factors which widen the breakthrough curve.

The mass transfer between gas- and solid-phases involves three kinetics steps: (1) an external kinetic: diffusion in the fluid layer surrounding the adsorbent grain. (2) An internal kinetic: diffusion in the particles porosity or sometimes in the metal. (3) A surface kinetic: adsorption or desorption at the metal surface.

A total time of mass transfer, t_m composed of three terms related to the three steps described previously could be defined as:

$$t_m = t_e + t_i + t_a$$

where t_e : external transfer time

$$t_e = \frac{Kdp}{6k_f} \text{ and } \frac{dpk_f}{D_m} = 2 + 1.8\text{Re}^{1/2}\text{Sh}^{1/3}$$

K : adsorption equilibrium constant, k_f : mass transfer coefficient (m/s), Re : Reynolds number, Sh : Sherwood number

t_i : internal transfer time

$$t_i = \frac{Kdp^2}{60D_c}$$

D_c : intraparticle diffusion coefficient (m^2/s)

t_a : adsorption time

$$t_a = \frac{(K - \beta)^2}{Kk_{\text{ads}}}$$

β : internal porosity, k_{ads} : adsorption constant rate (s^{-1}).

The Van Deemter coefficients have been identified:

Coefficient A .

$$A = dp$$

The experimental values obtained for alumina are in perfect agreement with the model which gives $A = dp$. But a slight divergence is observed for kieselguhr.

Coefficient B allows one to evaluate the packing material tortuosity τ .

$$B = 2D_m/\tau$$

D_m : molecular diffusion coefficient, τ : tortuosity.

The diffusion coefficient of D_2 in H_2 , $D_{\text{m H}_2\text{-D}_2} = 1.302 \text{ m}^2/\text{s}$ at 293 K and 1 bar. Tortuosity values obtained are summarized in Table 4. They are inferior to 1. These ones can be explained by the poor quality of the breakthrough curves and by the small number of experimental data.

Coefficient C refers to the mass transfer t_m . The different mass transfer times are detailed in Table 5.

Whatever the palladium content is, the chemical term of adsorption (t_a) seems to be the main limiting factor for kieselguhr. It is the same for alumina loaded at 20% palladium. For a 30% Pd alumina, it is impossible to identify the dominant kinetic, the different time have almost similar value.

4. Conclusions

Kieselguhr has been studied as a new support material for gas–solid chromatographic separation of hydrogen isotopes. It has been compared to the usual support: alpha-alumina. For both supports, palladium is impregnated as small dispersed particles in the 0.1 to 0.3 μm range diameter. For the same palladium loading, alumina is the most efficient packing material because of the higher Pd mass content per unit volume of the column.

Owing to the Van Deemter model, a fairly good optimization of the process was performed. In order to obtain more information about the different mass transfer times, thermoregulated separations are in

Table 4

Application of the Van Deemter equation to calculate the packing materials tortuosity

	$\text{Al}_2\text{O}_3 + 20\% \text{ Pd}$	$\text{Al}_2\text{O}_3 + 30\% \text{ Pd}$	Kieselguhr + 20% Pd	Kieselguhr + 30% Pd
τ	0.7	0.8	0.3	0.3

Table 5

Separation of a H₂ (93%)–D₂ (7%) mixture on alumina and kieselguhr coated with palladium

	Al ₂ O ₃ + 20% Pd	Al ₂ O ₃ + 30% Pd
Pd mass (g/cm ³ of column)	0.278	0.428
Mass transfer time t_m (s)	0.116	$5.89 \cdot 10^{-2}$
t_e (s)	$1.89 \cdot 10^{-3}$	$2.8 \cdot 10^{-2}$
t_i (s)	$3.8 \cdot 10^{-3} < t_i < 1.89 \cdot 10^{-3}$	$5.6 \cdot 10^{-3} < t_i < 2.8 \cdot 10^{-2}$
t_a (s)	$7.8 \cdot 10^{-2} < t_a < 9.3 \cdot 10^{-2}$	$2.9 \cdot 10^{-3} < t_a < 2.5 \cdot 10^{-2}$
	Kieselguhr + 20% Pd	Kieselguhr + 30% Pd
Pd mass (g/cm ³ of column)	0.113	0.207
Mass transfer time t_m (s)	$8.29 \cdot 10^{-2}$	0.108
t_e (s)	$1.07 \cdot 10^{-3}$	$1.95 \cdot 10^{-3}$
t_i (s)	$2.15 \cdot 10^{-4} < t_i < 1.07 \cdot 10^{-3}$	$3.9 \cdot 10^{-4} < t_i < 1.95 \cdot 10^{-3}$
t_a (s)	$8.07 \cdot 10^{-2} < t_a < 8.16 \cdot 10^{-2}$	$0.104 < t_a < 0.105$

progress. The expected results will be published soon.

References

- [1] E. Glueckauf, G.P. Kitt, Proceedings of Symposium on Isotope Separation, Amsterdam, North Holland, 1958, p. 210.
- [2] W.M. Rutherford, E. Ellis, G.C. Abell, Report of the Monsanto Research Corporation, January, 1988, reference MLM 3469 05245.
- [3] R. Lässer, K.H. Klatt, Phys. Rev. B 28 (1983) 22–28.
- [4] W.M. Rutherford, Mat. Sci. Forum 31 (1988) 19–38.
- [5] D.M. Ruthven, Fundamentals of Adsorption–Adsorption Kinetics and Adsorption Column Dynamics, Conf. 4–6 May 1986, Santa Barbara CA.
- [6] D. Tondeur, A. Glorius, M. Bailly, Chem. Eng. J. 23 (1982) 81–90.
- [7] V. Trentin, Thèse, Institut Polytechnique de Lorraine, 1993.
- [8] P. Schneider, J.M. Smith, AiChE J. 22 (1968) 762–771.
- [9] M. Suzuki, J.M. Smith, Chem. Eng. Sci. 26 (1971) 221–235.
- [10] J.J. Van Deemter, F.J. Zuiderweg, A. Klinkenberg, Chem. Eng. Sci. 5 (1956) 271–289.
- [11] J. Tranchant, Manuel Pratique de la Chromatographie en Phase Gazeuse, Masson, Paris 4th ed., 1995.
- [12] T. Paryjczak, Gas Chromatography in Adsorption and Catalysis, Ellis Horwood, Chichester, 1986.